Technetium-99m Methoxyisobutyl Isonitrile (RP30) for Quantification of Myocardial Ischemia and Reperfusion in Dogs

Quan-Sheng Li, Terry L. Frank, Dinko Franceschi,* Henry N. Wagner, Jr. and Lewis C. Becker

Division of Cardiology, Department of Medicine, and Division of Nuclear Medicine, Department of Radiology, Johns Hopkins Medical Institutions, Baltimore, Maryland

This study was done to determine whether [^{99m}Tc]methoxyisobutyl isonitrile (RP30), a nonredistributing myocardial perfusion agent, could be used to quantify regional myocardial blood flow distribution during ischemia and reperfusion, employing sequential injections of tracer, tomographic imaging, and appropriate image subtraction. Dogs underwent transient (6 min) coronary artery occlusion, followed by two paired injections of RP30 and radioactive microspheres combined with tomographic imaging, the first during coronary occlusion and the second after 60 min of reperfusion. To obtain a true image representative of reperfusion, the first set of images was corrected for ^{99m}Tc decay and subtracted from the second. During occlusion, tissue microsphere content and scintigraphic RP30 activity in the center of the ischemic region (both expressed as a fraction of the nonischemic region) were closely correlated, although RP30 consistently exceeded microsphere content (0.43 ± 0.03 vs. 0.24 ± 0.04, $p < 0.01$). Direct tissue counting of RP30 confirmed its relative excess in ischemic myocardium. Reperfusion was successful in 7/8 dogs, with an increase in RP30 activity to 0.98 ± 0.04 compared to 0.89 ± 0.03 for microspheres (p = N.S.). In one dog with microsphere-documented persistent ischemia, the RP30 defect was still present after reflow. Our results indicate that because of the lack of myocardial clearance and redistribution, repeat injections of RP30 can be used to quantify serial changes in regional myocardial blood flow.

J Nucl Med 29:1539–1548, 1988

Despite the clinical usefulness of thallium-201 (^{201}Tl) myocardial scintigraphy, it is generally recognized that ^{201}Tl is far from the ideal imaging agent. Its low-energy results in significant scatter and attenuation, impairing image quality and lesion contrast. In addition, its slow myocardial clearance and long physical half-life limit the permissible injected dose, resulting in count deficient images and heightened statistical noise.

Recently, a number of hexakis (isonitrile) technetium analogs have been introduced as possible substitutes for thallium-201 in the study of patients with suspected or proven coronary artery disease (*1–3*). These compounds have attracted considerable interest because of their flow-related distribution in the myocardium and the fact that they contain technetium-99m (^{99m}Tc), an abundant, cheap radionuclide with superior imaging characteristics using standard scintigraphic cameras. Technetium-99m methoxy isobutyl isonitrile ([^{99m}Tc] RP30) appears to represent the most promising agent of this type, since it is more rapidly cleared from the lung and has lower hepatic accumulation than other isonitrile compounds (*4,5*).

In contrast to ^{201}Tl, [^{99m}Tc] RP30 demonstrates minimal redistribution within the myocardium. Following an exercise study, ^{201}Tl activity falls in nonischemic regions ~ 50% in 4 hr, and rises in ischemic zones; however, little change has been observed over several hours with [^{99m}Tc] RP30 (*6–8*). This characteristic makes RP30 suitable for serial perfusion studies on the same day, using a split dose technique (*9,10*) and image subtraction to remove residual activity from earlier injections.

In this report we describe the use of [^{99m}Tc]RP30 to

Received Oct. 12, 1987; revision accepted Apr. 19, 1988.

For reprints contact: Lewis C. Becker, MD, Johns Hopkins Medical Institutions, Halsted 500, 600 N. Wolfe St., Baltimore, MD 21205.

*Present address: Cujetna Cesta 13, 41000 Zagreb, Yugoslavia.

quantitatively assess myocardial blood flow during ischemia and reperfusion in dogs with temporary coronary artery occlusion, applying the approach of serial injections of [^{99m}Tc]RP30 combined with appropriate image subtraction. To validate the scintigraphic estimates of blood flow, comparison was made with simultaneous injections of radioactive microspheres.

MATERIALS AND METHODS

Sterile, pyrogen-free RP30 was prepared from a kit provided by E.I. duPont Nemours and Company Biomedical Products. Twenty-five millicuries of [^{99m}Tc]pertechnetate in 0.1 to 3.0 ml was added to the kit, and the vial was placed in a boiling water bath for 15 min. After the vial had cooled, radiochemical purity was checked by chromatographic analysis (SEP-PAK). The radiochemical purity was > 95% in all cases.

To evaluate the potential of RP30 for serial imaging of myocardial blood flow, nine mongrel dogs of either sex weighing 40 to 60 lb were anesthetized, intubated, and ventilated with room air. Through a left thoracotomy, a pneumatic balloon occluder was placed around the proximal segment of either the left anterior descending coronary artery (LAD) (n = 6) or left circumflex coronary artery (LCX) (n = 3). The chest was then closed and lead II of the electrocardiogram was monitored continuously during the experiment.

The coronary artery was transiently occluded for a period of 6 min. One minute after the onset of occlusion, 5-8 mCi of [^{99m}Tc]RP30 were injected intravenously. At the same time, 2×10^6 gadolinium-153 (^{153}Gd) microspheres (DuPont Co. No. Billerica, MA) with a mean diameter of 16 μm were injected into the left atrium. Arterial blood samples were withdrawn by a Harvard pump at a constant rate of 2.16 ml/min, starting just before injection of the microspheres and continuing for 2 min afterwards, for calibration of the subsequent measurements of regional myocardial blood flow (*11*).

Tomographic imaging (TOMO-1) was begun 30 min after injection of the RP30 (25 min after release of the occlusion) and took ~ 30 min to complete. A second dose of [^{99m}Tc]RP30 (7-11 mCi) was injected immediately after the acquisition of TOMO-1 and 2×10^6 iodine-125 microspheres were injected simultaneously. A second tomographic imaging study (TOMO-2) was obtained, beginning 30 min after the injection of the second dose of RP30. The dog was immobilized throughout the two tomographic acquisitions.

In three additional dogs (two with LCX, one with LAD occlusion) only a single injection of RP30 and microspheres was made because of apparent lack of reperfusion in two animals (persistent ECG changes) and unexpected death before the second injection in the third. These animals were

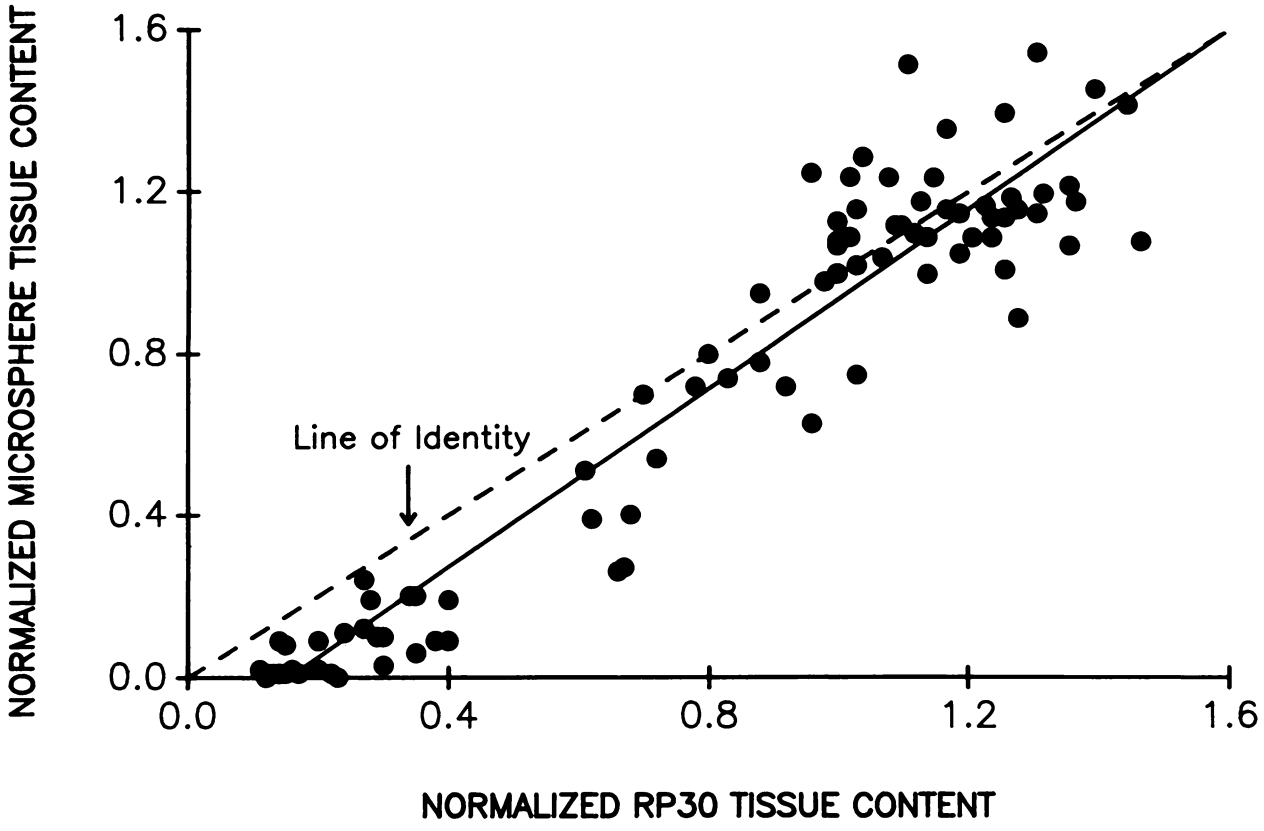

FIGURE 1
Correlation between normalized myocardial contents of RP30 and microspheres by direct tissue counting. Data represent 90 samples from two dogs with coronary artery occlusion and single injection of RP30. Solid line is line of regression (MS = −0.17 + 1.11 RP30, r = 0.96).

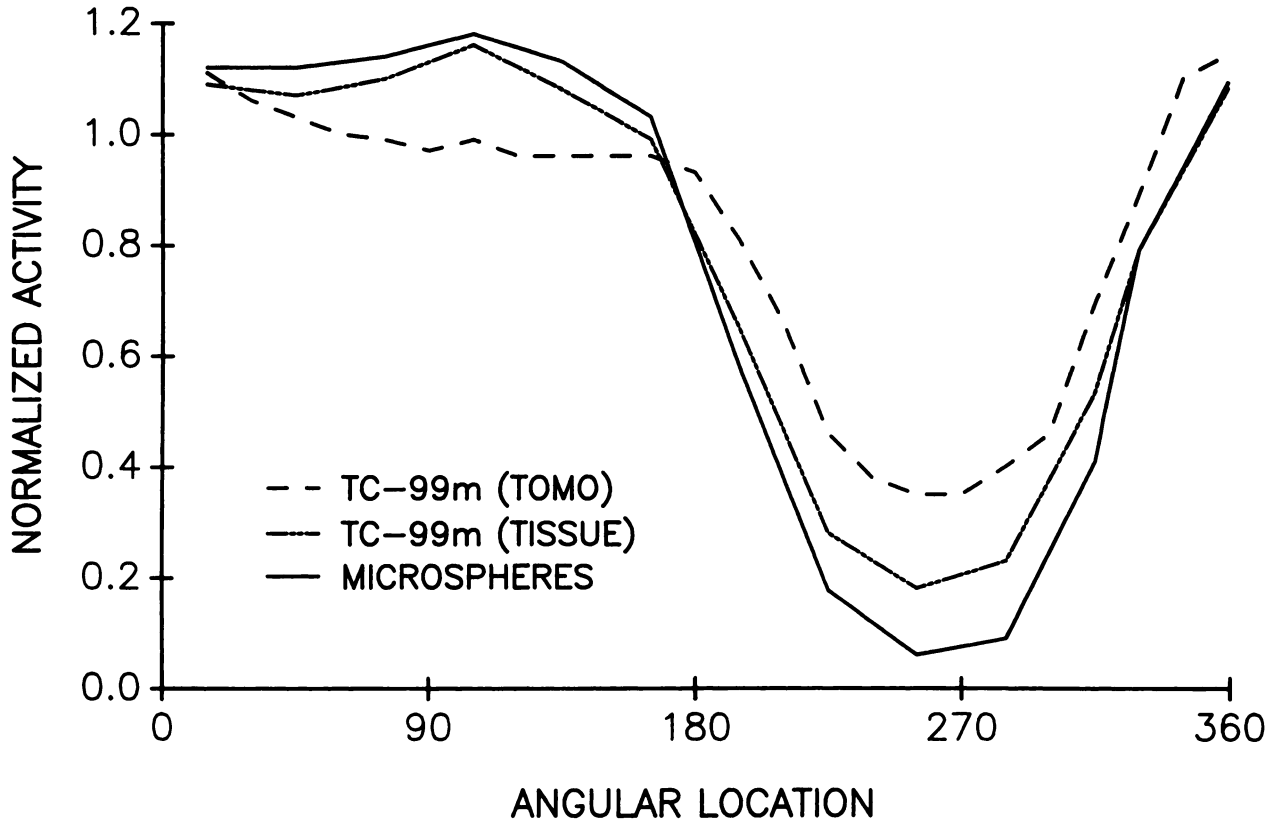

FIGURE 2
Averaged scintigraphic RP30, tissue RP30, and tissue microsphere activity curves for two mid left ventricular slices from three dogs with a single injection of RP30. Curves were aligned using the lowest and highest values in each slice. Mean values for the nadir were 0.06 for microspheres, 0.18 for tissue RP30, and 0.35 for scintigraphic RP30.

used to compare tissue content of RP30 and microspheres with scintigraphic uptake of RP30 in the ischemic zone.

Imaging was performed with a Technicare Omega 500 rotating large field-of-view camera, which acquired 60 30-sec images through 180° from the right lateral to the left lateral position. A high resolution parallel hole collimator was used, with a 20% energy window centered on the 140 keV gamma-ray peak. Raw images were obtained in 128 by 128 byte mode with a 1.4 camera magnification and a 20-cm radius of rotation. Transaxial slices were reconstructed using filtered back-projection with a Hanning 0.65 filter. The data were then reoriented to display six to seven serial short axis slices from apex to base of the left ventricle, equal in thickness (1 cm, 3 pixels) and perpendicular to the long axis.

Four short axis slices, representing the middle of the left ventricle, were displayed in 64 by 64 byte mode and subjected to a semi-automated analysis of regional myocardial RP30 content. The radial distribution of imaged RP30 activity was quantitated using a modification of the "CIRMAX" circumferential profile program provided by Technicare. As in the standard program, the operator generates a region of interest by positioning a circle just outside of the outer perimeter of the myocardial slice. For each angular interval (3°), the program finds the pixels which lie along the radial line at the desired angle, and determines the maximum count. The CIRMAX curve starts from 3 o'clock and proceeds counterclockwise. Unlike the standard program, however, the curve is normalized by the value located exactly 180° opposite the nadir of the curve, rather than by the highest value on the curve. This was done to provide comparability with the microsphere curves obtained by direct tissue counting.

To differentiate ischemic and nonischemic regions, monastral blue dye (1 ml/kg) was injected into the left atrium at the completion of imaging, following reocclusion of the coronary artery. The heart was then removed, the right ventricle excised, and the left ventricle was sectioned transversely from apex to base into six to seven slices (thickness 1 cm), corresponding to the number of short axis tomographic images. Each slice was then divided radially into 9-18 samples that were weighed and counted in a well-type scintillation counter after decay of ^{99m}Tc. Pulse height analysis was used to differ-

TABLE 1
Regional Myocardial Blood Flow (ml/min/100 g)*

	Occlusion	Reperfusion
Ischemic zone	15.9 ± 7.3	85.5 ± 20.3
Normal zone	91.0 ± 19.8	102.4 ± 19.8

* Values are mean ± s.d., based on 18 rings from five dogs.

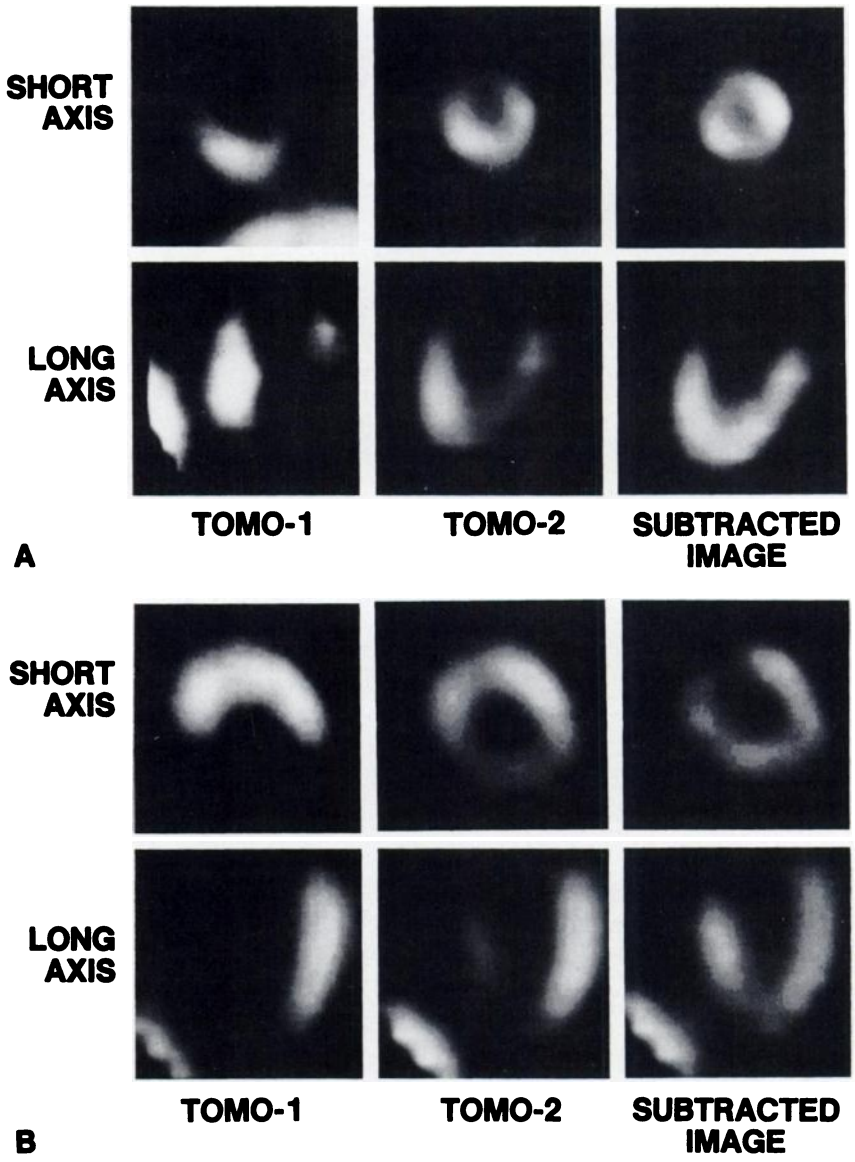

FIGURE 3
Effect of image subtraction on appearance of RP30 images following transient anterior descending (LAD) (Panel A) or circumflex artery (LCX) occlusion (Panel B) (Dog 2, ring 2 and Dog 4, ring 5, respectively). TOMO-1 represents RP30 distribution during occlusion. TOMO-2 was obtained after reperfusion and a second injection of RP30, but is "contaminated" by TOMO-1. The subtracted image represents TOMO-2 minus TOMO-1 corrected for ^{99m}Tc decay.

entiate activity from ^{153}Gd (62-120 keV) and ^{125}I (10-34 keV), with correction for energy crossover. In the three animals receiving only a single dose of RP30, samples were also counted for ^{99m}Tc on the first day and were recounted 2 days later for microsphere activity.

Regional myocardial blood flow (RMBF) was calculated using the formula: RMBF = R (Cm/Cr) (ml/min/g), where R = reference blood flow pump withdrawal rate, Cm = counts per gram in the myocardial samples, and Cr = counts in the entire reference blood sample. For each left ventricular slice, the RMBF of each sample was normalized by the RMBF of the sample located 180° away from the center of the ischemic zone, and expressed as a ratio.

To compare noninvasive tomographic imaging with actual tissue activity, corresponding images and tissue slices (which were of approximately equal thickness) were aligned, beginning from the apex. Alignment of corresponding scintigraphic and tissue curves began from 3 o'clock and proceeded in a counterclockwise direction.

TOMO-1 represented the distribution of blood flow during the period of occlusion, while TOMO-2 represented both the residual radioactivity from TOMO-1 as well as the distribution of [^{99m}Tc]RP30 during reperfusion. The residual radioactivity from TOMO-1 contributing to TOMO-2 was calculated by reducing the activity of each pixel in TOMO-1 by an amount corresponding to the physical decay of ^{99m}Tc occurring between TOMO-1 and TOMO-2. The decay corrected TOMO-1 image was then subtracted from TOMO-2 to yield a new image representing the true distribution of [^{99m}Tc] RP30 during reflow.

Results are expressed as the mean ± s.e.m. The statistical significance of mean differences between RP30 and microsphere activity curves were determined by the paired t-test. Regression analysis was used to determine the relation between RP30 and microsphere activities in the center of the ischemic zone in each animal as well as in multiple tissue samples from the dogs that had direct counting of tissue RP30 and microsphere activities.

TABLE 2
Comparison of RP30 and Microsphere Activity Curves

	Ischemia				Reperfusion					
	RP30 (TOMO-1)		Microspheres		RP30 (TOMO-2)		Subtracted TOMO		Microspheres	
Dog-ring	Nadir	Width†	Nadir	Width†	Nadir	Width†	Nadir	Width†	Nadir	Width†
1-2	0.39	183	0.06	196	0.83	0	1.38	0	0.90	0
-3	0.39	117	0.21	98	0.81	0	1.27	0	0.85	0
-4	0.38	96	0.09	146	0.75	0	1.09	0	1.05	0
-5	0.32	135	0.11	144	0.72	30	1.13	0	0.70	36
2-2	0.53	192	0.18	206	0.80	0	0.90	0	0.97	0
-3	0.46	165	0.15	225	0.84	0	1.05	0	0.79	0
-4	0.61	69	0.19	180	0.94	0	1.22	0	0.72	90
-5	0.85	0	0.21	111	0.84	0	1.30	0	0.72	28
3-3	0.29	192	0.17	277	0.58	99	0.85	0	0.72	55
-4	0.28	141	0.23	154	0.65	45	0.81	0	0.77	0
4-3	0.24	186	0.08	206	0.62	147	0.84	0	0.84	0
-4	0.27	174	0.14	135	0.73	21	0.92	0	1.03	0
5-2	0.44	192	0.29	131	0.60	84	0.75	0	0.89	0
-3	0.37	159	0.27	111	0.80	0	0.82	0	1.05	0
-4	0.44	87	0.34	68	0.95	0	1.03	0	0.89	0
-5	0.77	0	0.86	0	0.84	0	1.10	0	0.98	0
6-2	0.20	273	0.12	240	0.71	111	0.68	96	0.83	0
-3	0.25	168	0.06	160	0.61	132	0.75	0	0.88	0
-4	0.33	144	0.08	140	0.67	51	0.88	0	0.84	0
-5	0.63	69	0.37	40	0.79	0	0.77	0	0.81	0
7-2	0.60	108	0.76	0	0.92	0	1.10	0	1.28	0
-3	0.46	132	0.34	120	0.83	0	1.07	0	1.20	0
-4	0.39	162	0.20	180	0.79	0	0.97	0	0.83	0
-5	0.33	219	0.17	180	0.64	171	0.84	0	0.73	60
Mean	0.426‡	140	0.237	144	0.761‡	37.1*	0.980	4.0	0.886	11.2
s.e.m.	0.034	13.1	0.040	14.2	0.022	11.3	0.039	4.0	0.031	5.0

* $p < 0.05$ vs. corresponding microsphere value.
† "Width" refers to the length of the activity curve (expressed in degrees) falling below a threshold value of 0.75.
‡ $p < 0.01$.
Data represents all left ventricular rings analyzed from seven of the nine dogs. One dog with failed reperfusion and one dog without ischemia were not included in this Table but are included in Figure 8.

RESULTS

Comparison of tissue RP30 content and flow (microspheres) showed a linear relationship (MS = −0.17 + 1.11 RP30) with a high correlation coefficient (r = 0.96) (Fig. 1). Although agreement was good for normalized flows >0.4, a consistent excess of RP30 was observed for lower flow values. For normalized flows <0.4, RP30 content averaged 0.27 ± 0.03, compared with 0.10 ± 0.02 for flow. Scintigraphic RP30 activity was even higher than directly measured RP30 content in low flow regions (Fig. 2). Absolute values for blood flow obtained during the occlusion and reperfusion studies are shown in Table 1.

With respect to the imaging studies, image subtraction was found to be important for quantitation of flow during reperfusion. As demonstrated in Figures 3A and B, the residual activity from the first injection of RP30, (TOMO-1), "contaminated" the study obtained during reperfusion (TOMO-2) when image subtraction was not used. Despite the fact that more RP30 activity was injected for TOMO-2, the "shine through" phenomenon was clearly evident. However, after correction of TOMO-1 for physical decay of ^{99m}Tc and subtraction of this corrected image from TOMO-2, the new subtracted image demonstrated relatively homogeneous tracer distribution indicative of reperfusion. As shown in Table 2, the subtracted images provided significantly more accurate quantitation of defect severity and width compared to microspheres than did the non-subtracted TOMO-2 study.

The tomographic studies in which RP30 was injected during ischemia demonstrated clear-cut perfusion defects in the appropriate myocardial regions in all cases

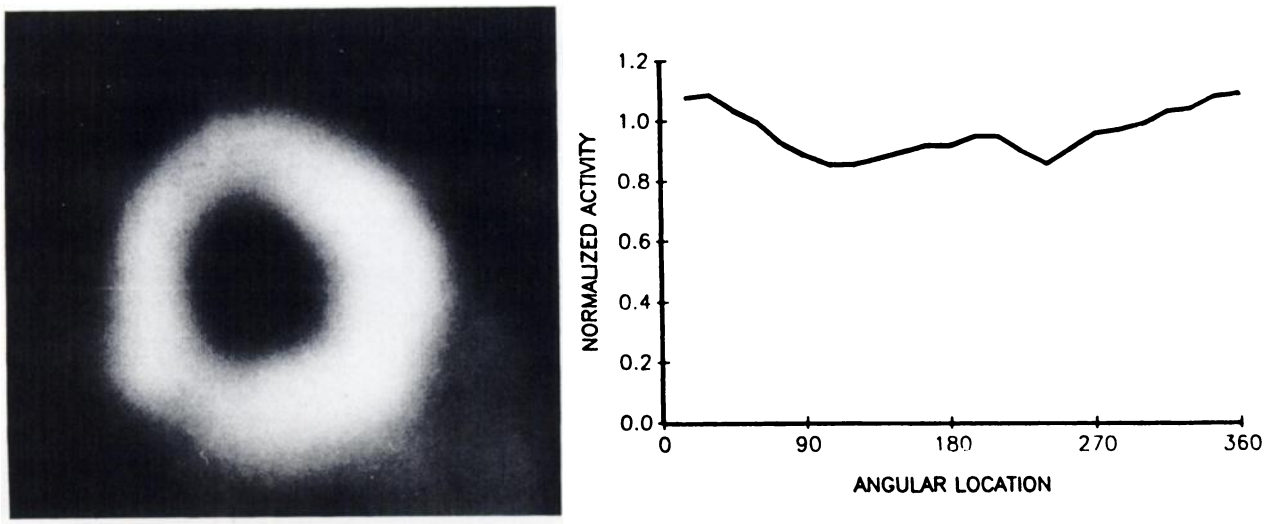

FIGURE 4
Short axis image from Dog 9 without significant ischemia by RP30 or microspheres.

in which microspheres verified ischemia. In one dog microsphere flow and RP30 images were both normal (Fig. 4). Two examples of dogs with perfusion defects are shown in Figures 5 and 6. Good agreement was found between the general shape of circumferential profile curves, representing normalized RP30 activity in short axis tomograms, and matched curves of normalized tissue microsphere content, after the curves were aligned as described in Methods. Figures 7A and C compare the average RP30 and microsphere activity curves from a mid-left ventricular slice (ring 3) during ischemia for dogs with LAD or LCX occlusion. Using a 75% threshold, the average width of the ischemic zone for all rings analyzed was not significantly different for RP30 and microspheres (140° vs. 144°, respectively; Table 2). However, normalized tomographic RP30 activity in the center of the ischemic zone was consistently higher than normalized tissue microsphere content (0.43 vs. 0.24, respectively, $p < 0.01$; Table 2). On the other hand, the correlation between the normalized activity ratio for RP30 and normalized microsphere ratio in the center of the ischemic zone was very high, with $r = 0.89$ (MS = −0.34 + 1.56 RP30, Fig. 8).

The studies in which RP30 was injected following reperfusion demonstrated reperfusion in seven of eight animals with initial defects (Fig. 5). One animal had persistent ischemia by RP30, as well as by microspheres (Fig. 6). In this dog, the normalized RP30 activity curve and microsphere curve showed good agreement (Figure 6, lower panel). As shown in Table 2, there was close agreement during reperfusion between quantitative RP30 and microsphere activities in the previously ischemic region (mean value 0.98 vs. 0.89, respectively, p = NS). The residual perfusion defect, using a 75% threshold, averaged 4.0° vs. 11.2°, respectively (p = N.S.). The correlation between mean RP30 and microsphere activities in the center of the previously ischemic zone in a mid left ventricular ring from each dog is shown in Figure 8. Within the relatively narrow range of normalized activity ratios in dogs with successful reperfusion (RP30, 0.68-1.38; microspheres, 0.83-1.28) there was no correlation between RP30 and microsphere values.

DISCUSSION

Our study demonstrates that myocardial ischemia and reperfusion may be imaged sequentially using [^{99m}Tc]RP30 and emission computed tomography, incorporating a split dose technique and image subtraction. The myocardial distribution of RP30 activity, quantified from short axis tomograms using a computerized circumferential profiles program, was shown to correspond to regional myocardial perfusion measured by radioactive microspheres. During ischemia, the correlation between normalized RP30 activity (from tomographic images) and microsphere content (from direct tissue counting) in the middle of the ischemic zone was excellent ($r = 0.89$), although the RP30 measurement was consistently higher and exceeded the microsphere value by an average of 80%. After release of the coronary occlusion, the tomographic images showed resolution of the perfusion defect in all animals in which reperfusion was successful and the mean normalized RP30 activity in the middle of the previously ischemic zone increased to 0.98 vs. 0.89 for microspheres.

The rationale for our split dose/image subtraction approach is dependent on the unique biodistribution and pharmacokinetic properties of [^{99m}Tc]RP30. Technetium-99m RP30 is a lipophilic cationic ^{99m}Tc complex which has been previously demonstrated in animal

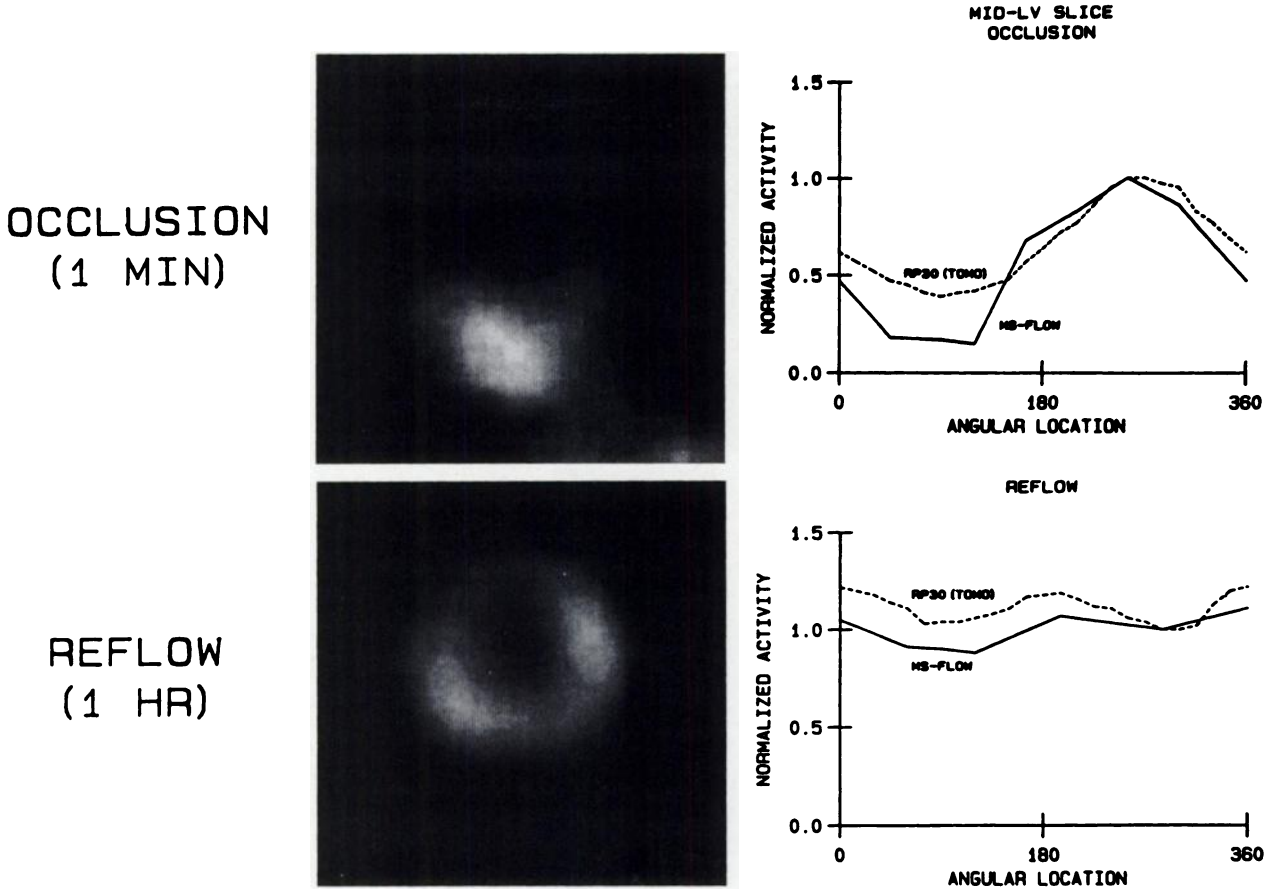

FIGURE 5
Panels represent short axis tomographic RP30 images along with corresponding quantitative CIRMAX curves (RP30 TOMO) and matched tissue microsphere activity curves (MS-FLOW) for occlusion (top) and reflow (bottom) in a dog with successful reperfusion (Dog 2, ring 2). Reflow image and curves represent subtracted data (see Fig. 3). Note marked perfusion defect during occlusion, with generally good agreement between tomographic RP30 and tissue microsphere curves except for overestimation of flow in ischemic zone by RP30. Reflow image shows partial resolution of the perfusion defect, confirmed by both RP30 and microsphere curves.

studies to accumulate in the myocardium in proportion to regional myocardial blood flow (*7,12,13*). Although the mechanism of uptake is unkown, cell fractionation studies have shown that 84% of RP30 can be found in the cytoplasm in association with a 10,000 D molecular weight protein (*14–16*). The clearance of RP30 from the myocardium has been found to be very slow (*8*). The effective half-life of RP30 in the myocardium has been shown to be similar to the physical half-life of ^{99m}Tc (*6,7,17*). Following the initial appearance of a perfusion defect, RP30 is felt to redistribute to an insignificant extent: the difference between activity in an ischemic zone and a normal zone remains nearly constant (*8*). RP30 has therefore been termed a "chemical microsphere". Because of this property, it becomes feasible to perform sequential imaging studies incorporating image subtraction to eliminate the effects of previous tracer injections on later images. Since redistribution and myocardial clearance are minimal, it should be necessary to correct earlier images only for isotope decay prior to subtraction.

The "split dose" sequential injection technique has been previously described for rest/dipyridamole planar ^{201}Tl imaging by Okada et al. (*9*). In that study, rest imaging was performed first and dipyridamole imaging second, using a larger dose for the second study. Because redistribution is relatively slow after rest injected studies (*18*), this approach was judged feasible. However, despite initially promising results, this technique has not become popular for ^{201}Tl scintigraphy, probably because of difficulties with precise image alignment (see below) and suboptimal count images with unacceptable statistical noise.

Our protocol called for a 30-min delay between RP30 injection and the start of tomographic imaging. Although the liver uptake of RP30 is less than that of other [^{99m}Tc]isonitriles, such as [^{99m}Tc]-t-butyl isonitrile (TBI) or [^{99m}Tc]carbomethoxyisopropyl isonitrile (CPI),

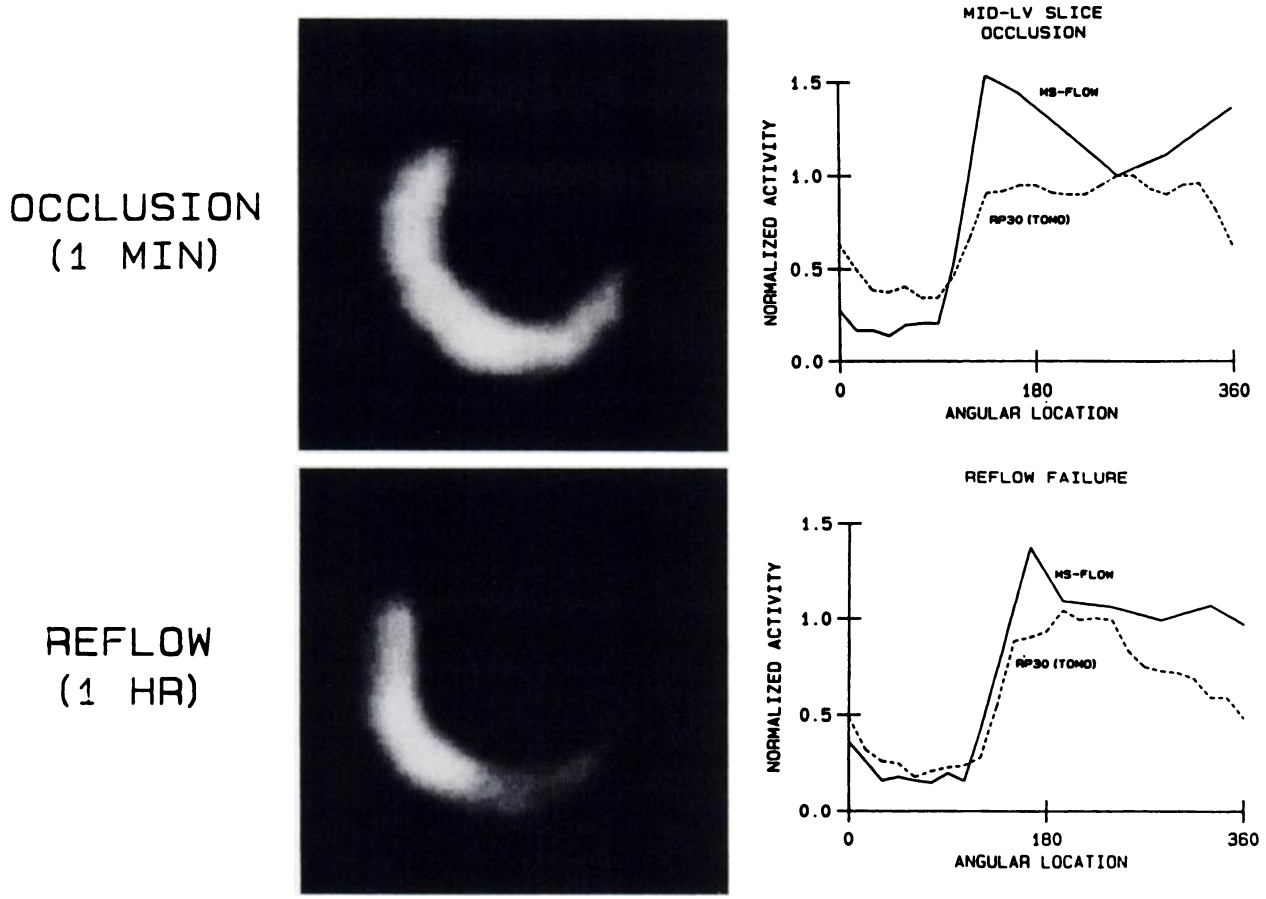

FIGURE 6
Images and curves in a dog with unsuccessful reperfusion (Dog 8, ring 3). Note persistence of marked perfusion defect after reflow, confirmed by tomographic RP30 and tissue microsphere activity curves.

considerable liver activity may still be seen initially. As activity clears from the hepatobiliary system, heart to liver activity ratios improve. The 30-min delay represents a compromise between optimal liver clearance and practical time constraints.

One of the most interesting findings of our study was that within the ischemic zone, RP30 activity measured from tomograms exceeded tissue microsphere content. There are at least two explanations for this finding. The first is related to the imaging. Because of the finite spatial resolution of the Anger camera, as well as photon scatter, RP30 images of the heart in situ demonstrate a reduction in lesion contrast compared to the real activity distribution (*19,20*) (Fig. 2). Microsphere measurements on the other hand, are not subject to this error because they are made from direct counting of tissue samples. The second explanation, as shown by our own data, is that tissue RP30 content is higher than tissue microsphere content (Figs. 1, 2). Based on the data of Leppo et al. in the isolated blood perfused rabbit heart (*21*) and our own values for myocardial blood flow (Table 1), the first pass extraction of RP30 in ischemic myocardium should have been ~ 50%, compared to 40% in normal myocardium (ratio, ischemic to normal = 1.2). Microspheres, on the other hand, have an extraction ratio close to 100% (ischemic/normal zone ratio = 1.0). The higher ratio of ischemic to normal zone extraction for RP30 may have been responsible for the relative excess of RP30 present in the ischemic zone.

The successful clinical application of this approach will depend on precise image alignment to permit subtraction without creation of artifactual defects. For the current study, image alignment was not a problem because the dogs were anesthetized and immobilized. In the clinical setting, however, it will not be possible to keep a patient immobile long enough to perform sequential injections and imaging studies, and although patient positioning systems using laser light beams may help, they will probably be insufficient. Both operator interactive and automated computer methods have been described for alignment of planar images (*22,23*). An automated technique, which has been adapted to tomographic images, utilizes fast Fourier transformation and maximization of a cross-correlation function (*24*). We have developed a new method for motion artifact correction of tomographic studies which may also be adapted for this purpose (*25*). The center of the

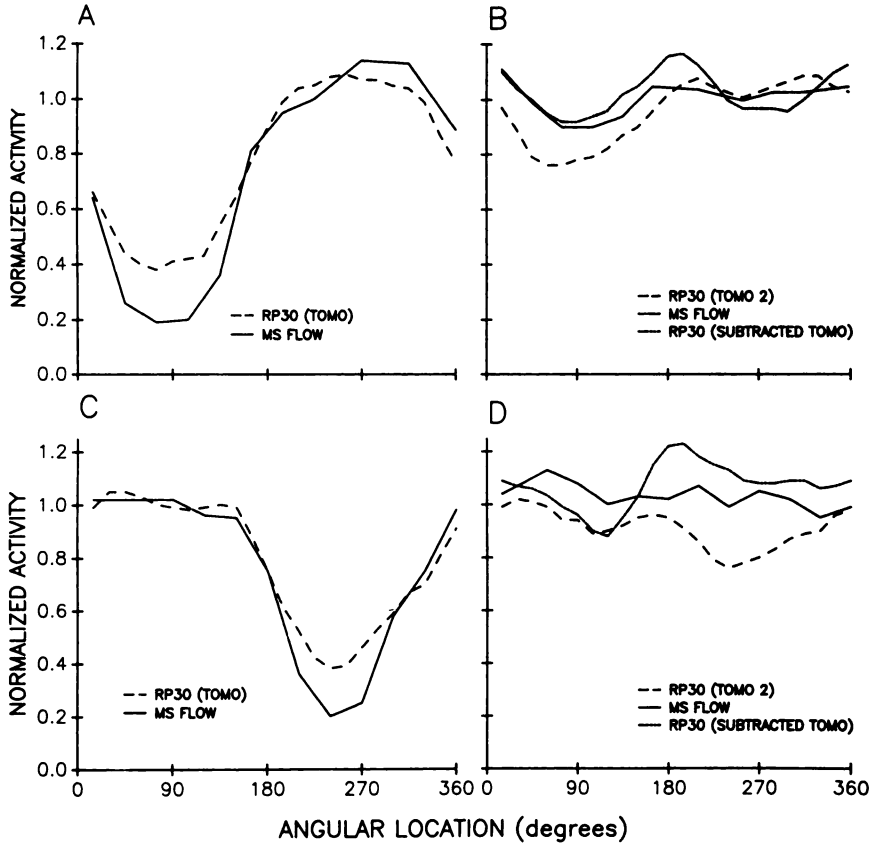

FIGURE 7
Averaged RP30 and microsphere activity curves for a mid-left ventricular slice from four dogs with anterior descending coronary artery occlusion (panel A) and reflow (panel B), and three dogs with circumflex artery occlusion (panel C) and reflow (panel D). RP30 curves were obtained from tomograms and microsphere curves from tissue counting. TOMO 2 shows residual perfusion defect due to "contamination" from first RP30 study. Subtracted TOMO provides better estimate of flow distribution during reperfusion.

left ventricle is tracked automatically in each projection image and the whole projection image is shifted prior to reconstruction so that the heart center conforms to the expected position of an arbitrary fixed point in space. If images obtained sequentially are shifted so that the center of the left ventricle in each study represents the same point in space, it should be possible to perform image subtraction without production of perfusion artifacts.

ACKNOWLEDGMENTS

The authors thank Anthony F. DiPaula, Jon Clulow, Hayden T. Ravert, and Christine G. Holzmueller for their assistance.

This work was supported by U.S. Public Health Service Grant No. 17655-12 (SCOR in Ischemic Heart Disease) from The National Heart, Lung, and Blood Institute, and a gift from Mary L. Smith of the W.W. Smith Charitable Trust, Rosemont, PA.

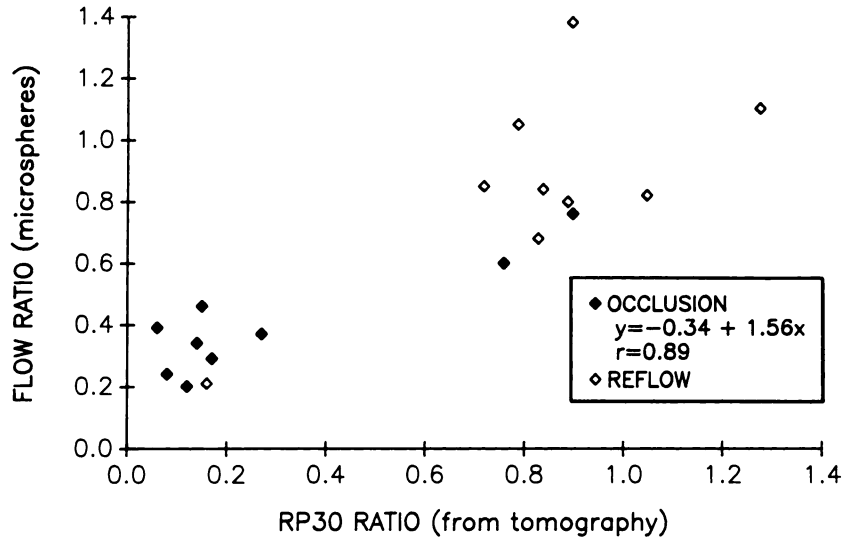

FIGURE 8
Normalized RP30 activity from tomographic images vs. microsphere flow from matched tissue samples in center of ischemic zone. Each data point represents a single animal. Data were taken from the left ventricular ring showing most severe ischemia in each animal. Reflow RP30 values were obtained from the same location where most severe ischemia was identified in initial images.

REFERENCES

1. Jones AG, Abrams, MJ, Davison A, et al. Biological studies of a new class of Technetium complexes: the hexakis (alkylisonitrile) technetium (I) cations. *Int J Nucl Med Biol* 1984; 11:225–234.
2. Holman BL, Campbell CA, Lister-James J, et al. Effect of reperfusion and hyperemia on the myocardial distribution of technetium-99m t-butylisonitrile. *J Nucl Med* 1986; 27:1172–1177.
3. Holman BL, Sporn V, Jones AG, et al. Myocardial imaging with technetium-99m CPI: initial experience in the human. *J Nucl Med* 1987; 28:13–18.
4. McKusick K, Holman BL, Jones AG, et al. Comparison of 3 Tc-99m isonitriles for detection ischemic heart disease in humans [Abstract]. *J Nucl Med* 1986; 27:878.
5. McKusick KA, Holman BL, Rigo P, et al. Human myocardial imaging with 99m-Tc isonitriles [Abstract]. *Circulation* 1986; 74: II-296.
6. Williams SJ, Mousa SA, Morgan RA, et al. Pharmacology of Tc-99m-isonitriles: agents with favorable characteristics for heart imaging [Abstract]. *J Nucl Med* 1986; 27:877.
7. Mousa SA, Stevens SJ, Williams SJ. Regional distribution of Tc-99m hexakis-aliphatic isonitriles in ischemic hearts with and without reperfusion [Abstract]. *J Nucl Med* 1986; 27:994.
8. Okada RD, Glover D, Gaffney T, et al. Myocardial kinetics of technetium-99m-hexakis-2-methoxy-2-methylpropyl-isonitrile. *Circulation* 1988; 77:491.
9. Okada RD, Lim YL, Rothendler J, et al. Split dose thallium-201 dipyridamole imaging: a new technique for obtaining thallium images before and immediately after an intervention. *JACC* 1983; 1:1302–1310.
10. Stirner H, Buell U, Kleinhans E, et al. Tc-99m hexakis-(2-methoxy-isobutyl-isonitrile) (RP-30) vs Tl-201. A quantitative comparison with SPECT in coronary heart disease (CHD) [Abstract]. *J Nucl Med* 1987; 28:620.
11. Domenech RJ, Hoffman JIE, Noble MIM, et al. Total and regional coronary blood flow measured by radioactive microspheres in conscious and anesthetized dogs. *Circ Res* 1969; 25:581–596.
12. Mousa SA, Cooney JM, Williams SJ. Regional myocardial distribution of RP-30 in animal models of myocardial ischemia and reperfusion [Abstract]. *J Nucl Med* 1987; 28:620.
13. Canby RC, Pohost GM. Dependence of the distribution of a technetium isonitrile on myocardial viability after an ischemic insult [Abstract]. *Circulation* 1986; 74:II-296.
14. Mousa SA, Williams SJ. Myocardial uptake and retention of Tc-99m-hexakis-aliphatic isonitriles: evidence for specificity [Abstract]. *J Nucl Med* 1986; 27:995.
15. Mousa SA, Maina M, Brown BA, et al. Retention of RP-30 in the heart may be due to binding to a cytosolic protein [Abstract]. *J Nucl Med* 1987; 28:619.
16. Mousa SA, Maina M, Williams SJ. Myocardial uptake and retention of Tc-99m-RP-30: evidence for specificity [Abstract]. *Circulation* 1986; 74:II-513.
17. McKusick K, Bellar G, Berman D, et al. Initial clinical results with Tc-99m methoxy isobutyl isonitrile [Abstract]. *JACC* 1987; 9:28A.
18. Murphy FL, Maddahi J, Train KV, et al. Thallium-201 uptake and washout at rest vs. exercise in patients without coronary artery disease-implications for quantitation [Abstract]. *JACC* 1983; 1:601.
19. Caldwell JH, Williams DL, Hamilton GW, et al. Regional distribution of myocardial blood flow measured by single-photon emission tomography: comparison with in vitro counting. *J Nucl Med* 1982; 23:490–495.
20. Chang W, Henkin RE, Buddemeyer E. The sources of overestimation in the quantification by SPECT of uptakes in a myocardial phantom: concise communication. *J Nucl Med* 1984; 25:788–791.
21. Leppo JA, Moring AF. An evaluation of a technetium-labelled isonitrile analog as a myocardial imaging agent and comparison to thallium [Abstract]. *Circulation* 1986; 74: II-297.
22. Williams DL, Ritchie JL, Hamilton GW. Implementation of a digital image superposition algorithm for radionuclide images: an assessment of its accuracy and reproducibility. *J Nucl Med* 1978; 19:316–319.
23. Appledorn CR, Oppenheim BE, Wellman HN. An automated method for the alignment of image pairs. *J Nucl Med* 1980; 21:165–167.
24. Eisner RL, Noever T, Nowak D, et al. Use of cross-correlation function to detect patient motion during SPECT imaging. *J Nucl Med* 1987; 28:97–101.
25. Links JM, Geckle WJ, Frank TL, et al. Correction for patient and cardiac movement in exercise thallium SPECT [Abstract]. *J Nucl Med* 1987; 28:630.